Extended Abstracts of the 22nd (1990 International) Conference on Solid State Devices and Materials, Sendai, 1990, pp. 31-34

B-1-5

Effect of Reservoir in Electrodes on Double Barrier Resonant Tunneling

Akira Sugimura

NTT Basic Research Laboratories
Musashino-shi, Tokyo 180, Japan

Effects of reservoir in electrodes on double barrier tunneling structures are investigated theoretically. It is found that there is a quantum transition region around the boundary between the quantum transport and the reservoir regions. The double barrier tunneling can be considered as a coherent effect when the electron transfer rate t is larger than the damping rate γ, while it is a sequential tunneling process when γ dominates over t. It is also found that the best frequency response can be obtained in the structure $\gamma \sim t$.

I. Introduction

Tunneling phenomena in double barrier diode structures[1] have been attracting much interest both theoretically[2,3,4] and experimentally[5]. Although the tunneling is a quantum mechanical phenomena, effects of reservoir on this system, which determines electron coherence, have not been considered sufficiently. Whether the double barrier tunneling is a coherent effect or a sequential tunneling is still controversial. In the present paper, we theoretically make clear the reservoir effects on the coherence and dynamic properties of the resonant tunneling.

II. Quantum transition approach

We propose a new theoretical approach, which is based on the fact that the electrons are separated to three regions I, II and III as shown in Fig.1. The electron states are described by the Liouville equation for the density operator ρ, which is represented by the eigen states of the localized electrons in each regions as basis functions. The coherent motion of ρ is then determined by the Hamiltonian,

$$\begin{aligned} H_{coh} &= -\sum_{1}(T_R a_1^\dagger a_2 + h.c.) - \sum_{3}(T_L a_2^\dagger a_3 + h.c.) \\ &+ \sum_{1} \varepsilon_1 a_1^\dagger a_1 + \varepsilon_2 a_2^\dagger a_2 + \sum_{3} \varepsilon_3 a_3^\dagger a_3, \qquad (1) \end{aligned}$$

where a_i, $a_i^\dagger$, and ε_i (i=1,2,3) are annihilation operator, creation operator and electron energy

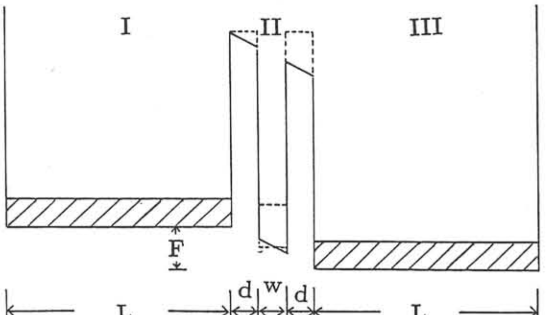

Fig.1: Schematic band diagram for the double barrier resonant tunneling diode. I and III are electrode regions with lengths of L. II is a quantum well region. Broken lines indicate the approximated potential profile used in the calculation.

in respective regions. T_R and T_L are transfer energies. We here assume that the electrons in electrodes I and III are subjected to different reservoirs and are thermalized differently, while electrons in II are not directly affected by any reservoirs. These reservoir interactions give rise to the damping of $\rho_{i,j}$ to its locally equilibrium states with a damping constant $\gamma_{i,j}$. The motion of $\rho_{i,j}$ is then expressed by,

$$\frac{d\rho_{i,j}}{dt} = \frac{i}{\hbar}[H_{coh}, \rho]_{i,j} + \gamma_{i,j}(F_i\delta_{i,j} - \rho_{i,j}), \qquad (2)$$

where F_i is a quasi Fermi distribution functions of electrons in each region. According to Eq.(2), we can see that the double barrier tunneling is similar to the quantum transition from the excited states of the three energy level system to the ground state as shown in Fig.2. Tunneling currents are related to the off-diagonal elements $\rho_{1,2}$ and $\rho_{2,3}$, which correspond to dipole operators in the three level system. For simplicity we restrict ourselves to the case where $\gamma_{11} = \gamma_{33} = \gamma$ and $\gamma_{22} = 0$. Then we get the relations $\gamma_{12} = \gamma_{23} = \gamma/2$ and $\gamma_{13} = \gamma$. Since Eq.(2) is a linear equation system, we can solve it straightforwardly to give the coherence properties of the tunneling phenomena.

III. Coherence properties

In the Wigner function approach[3,4] for the resonant tunneling phenomena, reservoir effects were taken into account by using "boundary conditions." However, the boundary between the quantum transport region and the reservoir region is not clear. Detailed electronic structure around the boundary is, therefore, investigated. In the present paper, calculations were made for GaAs/$Al_{0.3}Ga_{0.7}As$ resonant tunneling diode with well and barrier widths of 50 and 30 Å, respectively. Figure 3 shows the electron density distribution near the barrier in the electrode I. Electrons are accumulated around the boundary. In addition to this, quantum oscillation is seen when the resonant tunneling condition is fulfilled (F = 200 mV). Figure 4 shows electron local currents in I, which exhibit spatially non-uniform behavior near the barrier. This result indicates that the electrons are moved from the electrode region I to the quantum well re-

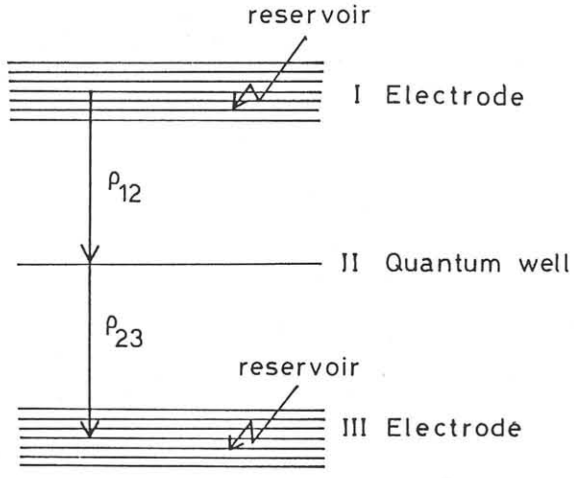

Fig.2: Diagram of the three level system corresponding to the double barrier resonant tunneling. The excited state I and the ground state III are subjected to different reservoirs.

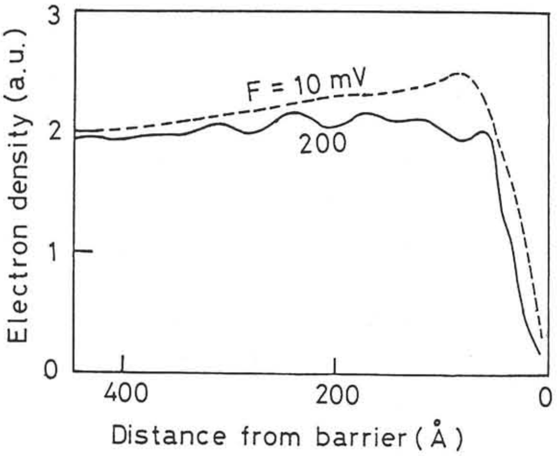

Fig.3: Electron density distribution near the barrier inside the electrode for AlGaAs/GaAs resonant tunneling diode. Resonance condition is almost fulfilled when the applied electric fields F is 200 mV, while it is not when F = 10 mV.

gion II not by the classical electron flow but by the non-local quantum transition. Oscillations in Figs. 3 and 4 are caused by the interference of the electron wave in the double barrier. The damping of this oscillation in the electrode I is determined by the damping constant γ_{12} for the off-diagonal element of ρ. Thus, we can say that there exists a quantum transition region near the boundary inside the reservoir region. The coherent interaction length L_c can then be defined by the size of the quantum transition region. Figure 5 shows the correlation function for electrons near the barrier in I. The larger value for the damping rate γ causes the decrease of the electron coherence, which gives rise to the decrease of L_c. According to the above results, it is seen that, since the resonant tunneling is a quantum mechanical, non-local phenomenon, we cannot expect abrupt transition from the quantum transport region to the reservoir region. In analyzing quantum transport phenomena, we must take into account the existence of the quantum transition region inside the reservoir, where both coherent and incoherent interactions are occurring simultaneouly.

The static tunneling current shows resonance curve with respect to the applied electric field. The peak tunneling current of the resonance curve and its resonance width are calculated as shown in Fig.6 as a function of the damping constant γ. In the smaller γ region, peak current is constant. Tunneling in this region is considered to be a coherent resonant tunneling. When γ exceeds around $10^{13}\mathrm{sec}^{-1}$, which corresponds to the electron transfer rate t ($\sim T_L/\hbar \sim T_R/\hbar$) in the present structure, the peak current decreases and the resonance width increases. This corresponds to a partially incoherent, sequential tunneling region. It is worth while noting that the incoherence of the tunneling stems from the reservoir interaction outside the quantum well through non-local effect of the electron transport. A transition occurs from a coherent tunneling region to a sequential tunneling region, when γ is comparable to the electron transfer rate t.

From the device application stand point, frequency response is very important, which is also affected significantly by the reservoir interac-

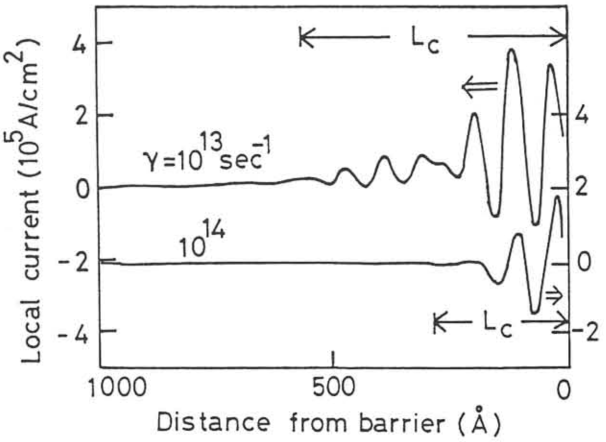

Fig.4: Electron local currents near the barrier in the electrode for AlGaAs/GaAs resonant tunneling diode. Coherent interaction region L_c is a size of the quantum transition region, where the local current is oscillating. When the damping rate γ increases, L_c decreases.

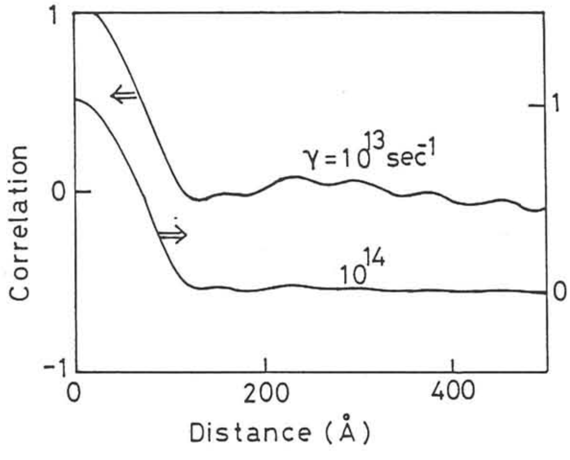

Fig.5: Correlation function for the electron near the barrier in electrode I. γ is a damping rate.

tion. A small signal frequency response is calculated by linearizing the time dependent Liouville equation given in Eq.(2). Figure 7 shows the frequency response characteristics when the bias voltage is fixed to 200 mV for different damping rates γ. A resonance in modulation frequency exists at around several THz. This value corresponds to the electron transfer rate t. The widest bandwidth can be obtained when γ is near to t.

IV. Conclusion

A new theoretical approach for the analysis of the double barrier resonant tunneling is proposed, which is suitable to reveal the coherence properties of the tunneling electrons. Using this method, effects of reservoir in electrodes are investigated. It is found that there is a quantum transition region with a length of L_c around the boundary between the quantum transport region and the reservoir region. The double barrier tunneling can be considered as a coherent effect when the electron transfer rate t is larger than the damping rate γ. When γ dominates over t, sequential tunneling process increases and the peak tunneling current decreases. It is also found that the best frequency response can be obtained in the structure $\gamma \sim t$.

References

1) R. Tsu and L. Esaki; Appl. Phys. Lett. **22**(1973) 562.

2) B. Ricco and M. Ya. Azbel; Phys. Rev. B**29**(1984) 1970.

3) W. Frensley; Phys. Rev. Lett. **57**(1986) 2853.

4) W. Frensley; Phys. Rev. B**36**(1987) 1570.

5) T. Sollner et al.; Appl. Phys. Lett. **43**(1983) 588.

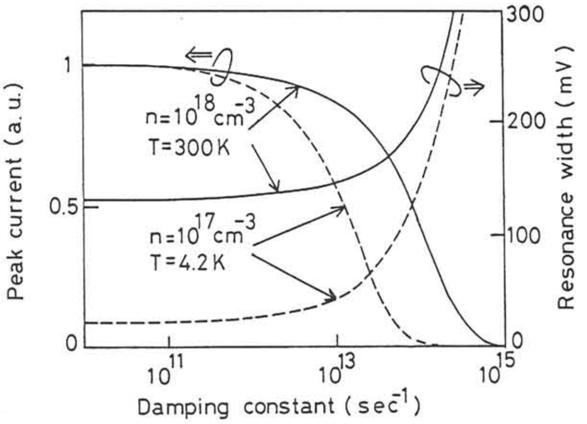

Fig.6: Peak current and resonance width of the resonance curve for the static I-V characteristics of the AlGaAs/GaAs resonant tunneling diode as a function of the damping rate γ. Averaged carrier densities inside the electrodes are assumed to be $10^{18}cm^{-3}$ (solid line) or $10^{17}cm^{-3}$ (broken line). Ambient temperature, which determines electron distribution in the electrodes, is 300K (solid line) or 4.2K (broken line).

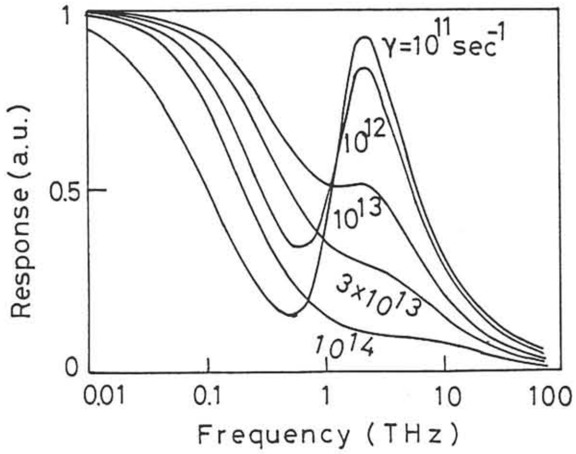

Fig.7: Small signal frequency response characteristics for the resonant tunneling diode with different damping rates γ. Bias electric field is 200 mV, which fulfills the condition of the negative differential resistance.